Micropatterning

DOI: 10.1002/anie.200900807

Microscale Control of Stiffness in a Cell-Adhesive Substrate Using Microfluidics-Based Lithography**

*Yuk Kee Cheung, Evren U. Azeloglu, David A. Shiovitz, Kevin D. Costa, Dror Seliktar, and Samuel K. Sia**

In native tissues, the rigidity of the microenvironment provides important mechanical cues in directing cellular processes, including adhesion, spreading, migration, cytoskeletal organization,[1–4] growth, differentiation, apoptosis,[5–7] and tissue morphogenesis.[8,9] In particular, microscale variations in stiffness (with Young's modulus ranging from 100 Pa to 1 MPa) have been observed over length scales ranging from subcellular (< 5 μm) to multicellular (> 300 μm) dimensions in healthy and diseased tissues of the brain,[10] bone,[11,12] heart,[13] and cartilage.[14] Moreover, recent evidence suggests that heterogeneous distribution of mechanical properties is responsible for the spatial organization and differentiation of different germ layers during embryogenesis.[15]

Previously, most attempts to reconstruct microscale variations in substrate stiffness have used collagen-coated polyacrylamide gels, in which the stiffness can be tuned by varying the amount of bisacrylamide cross-linker. In constructing a single-step[3,16] or a continuous[17,18] gradient in substrate stiffness, these studies demonstrated a range of cellular behavior, most notably durotaxis (that is, the guidance of cell migration by microscale variations in substrate stiffness), with cells migrating from compliant toward stiff regions. To recapitulate the myriad microscale variations of stiffness in native and diseased tissues, it will be important to develop a technology for constructing a cell-adhesive substrate that exhibits a flexible spatial architecture with controllable local variations that are not limited to monotonic or single-step stiffness changes.

Previously, we and others developed microfluidics-based lithography techniques[19] (in which the fabrication of 3D gels was performed inside a microchannel) to pattern multiple 3D gels aligned to each other (Figure 1).[20–22] Unlike other lithography techniques inside a microchannel, where particles are gelled in solution and flow away,[23] our technique can produce aligned, multicomponent microstructures that adhere to the underlying substrate. Herein we extend this microfluidics-based lithography technique to pattern a substrate made of materials that promote cell adherence, spreading, and migration and exhibit well-defined variations in stiffness, which we measure directly using atomic force microscope (AFM) indentations. An advantage of this approach is that the patterned spatial variation of stiffness can be highly versatile, and is not limited to binary or simple linear changes in stiffness. Thus, we aim to demonstrate the use of microfluidics-based lithography for researchers in cell biology and tissue engineering interested in recreating a heterogeneous 3D extracellular matrix (ECM) to high precision.

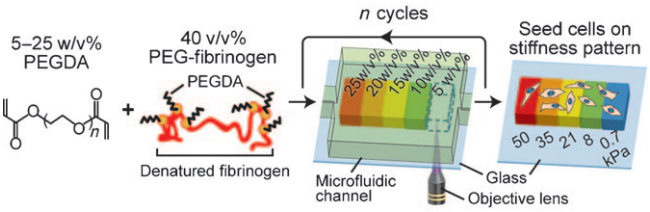

Figure 1. Experimental setup for microfluidics-based lithography to micropattern cell-adhesive substrates with defined heterogeneities in stiffness. Prepolymer solutions were prepared by adding various w/v% of PEGDA to a fixed amount of PEG-fibrinogen, whose synthesis involves crosslinking PEGDA to free thiol groups (depicted as circles) present on the denatured bovine fibrinogen. During each cycle, a prepolymer solution was drawn into a microfluidic channel where it was photocrosslinked into hydrogel blocks. The photo-cross-linking of a hydrogel containing 5 w/v% of PEGDA for a hypothetical structure in the fifth cycle is shown. At the end of fabrication, the microfluidic channel was peeled away to expose the stiffness patterns for stiffness measurement and cell seeding.

To control the stiffness of the hydrogel we varied the chain length and concentration of polyethylene glycol diacrylate (PEGDA) oligomers in the prepolymer. To promote cell adhesion, spreading, and migration we supplemented the prepolymer with a constant amount of PEG monoacrylate-linked bovine fibrinogen (PEG-fibrinogen).[24] This biosynthetic oligomer provides a uniform density of integrin-binding sites and can be photo-cross-linked using its acrylate side chains (Figure 1). As in other cell-adhesive PEG-protein hydrogels (such as RGD peptides covalently attached to PEG),[25–27] PEG-fibrinogen (ca. 5 mg mL^{-1}) provides ample cell-binding sites, and large amounts of fibrinogen can be produced with simple protein purification techniques.[24] Also,

[*] Y. K. Cheung, Dr. E. U. Azeloglu, D. A. Shiovitz, Prof. K. D. Costa, Prof. S. K. Sia
Department of Biomedical Engineering, Columbia University
1210 Amsterdam Ave, New York, NY 10027 (USA)
Fax: (+1) 212-854-8725
E-mail: ss2735@columbia.edu
Prof. D. Seliktar
Biomedical Engineering Department
Technion-Israel Institute of Technology
Technion City, Haifa 32000 (Israel)

[**] This work is supported by a Scientist Development Grant (to S.K.S) from the American Heart Association, NSF CAREER award (to S.K.S and K.D.C.), and a Croucher Foundation Scholarship (to Y.K.C). We also thank Benjamin W. Lee for helping with data analysis.

Supporting information for this article is available on the WWW under http://dx.doi.org/10.1002/anie.200900807.

like many other cell-adhesive and degradable hydrogels, PEG-fibrinogen has previously not been shown to be a basis material for direct micropatterning inside a microchannel,[20] where the acute requirements of both high control in fabrication and high cell adhesion and viability are often incompatible (for example, high concentrations of photoinitiator allow faster photopolymerization but can be cytotoxic).

To use the microfluidics-based lithographic technique to pattern cell-adhesive microstructures, we first tested the use of an epifluorescence microscope as the light source for photopolymerization of PEG-fibrinogen-based structures. With an epifluorescence exposure system, the size and shape of the cell-adhesive microstructure patterned during each cycle are limited by the power of the objectives and the geometry of the field diaphragm[20] (in this case, the field diaphragms were rectangles of 150 to 1400 μm, with an aspect ratio of 1 to 1.4). We overcame these limitations by overlapping the exposure window on portions of the microstructures formed in previous cycles; in this manner, we could achieve the micropatterning of discrete stiffness gradients containing multiple adjoining hydrogel blocks (Figure 2a), with step sizes as small as 27 μm (Supporting Information, Figure S1). As an alternative exposure system, we demonstrated the use of a confocal laser scanning microscope to pattern PEG-fibrinogen with discrete variations of stiffness, featuring adjoining and free-standing hydrogel blocks of linear and curved geometries, and spanning a variety of scales (Figure 2c). Furthermore, by using a scanning laser as an exposure source, we could achieve spatial control of stiffness patterns to less than 13 μm (Supporting Information, Figure S2).

Bulk measurements of stiffness are often used as an estimate of microstiffness; however, these measurements do not always correspond to the true microstiffness of micropatterned gels. This discrepancy can be due to the change in stiffness that accompanies the rate of reaction of the UV cross-linkers,[18] and the diffusion of radicals between adjoining hydrogel blocks during photopolymerization. We sought to measure the stiffness of our micropatterned PEG-fibrinogen hydrogels directly using AFM indentations conducted in force mode.[28] We analyzed each indentation force-response curve (inset in Figure 2b) with a pointwise method, such that the depth-dependent apparent elastic modulus was computed as a function of indentation depth. Our AFM results confirmed a discrete stiffness gradient that ranged from 0.7 to 50 kPa (Figure 2b) over a distance of 660 μm, with a constant step size of (130 ± 1) μm (Figure 2a). We also observed minimal stiffness variation within each section of the discrete gradient, as intended (standard deviations ranged from 0.2 to 2.4 kPa). Given that cell adhesion and migration can be influenced by the topography of the adhering substrate, we performed contact mode AFM imaging to characterize the surface topography and roughness of the discrete stiffness gradient. We observed an average surface roughness of 86 nm among hydrogels with 10–25 w/v% of PEGDA (Figure 2d and Supporting Information, Figure S3a-b). Therefore, the height along each stiffness section is effectively uniform, with variations of approximately 5 μm

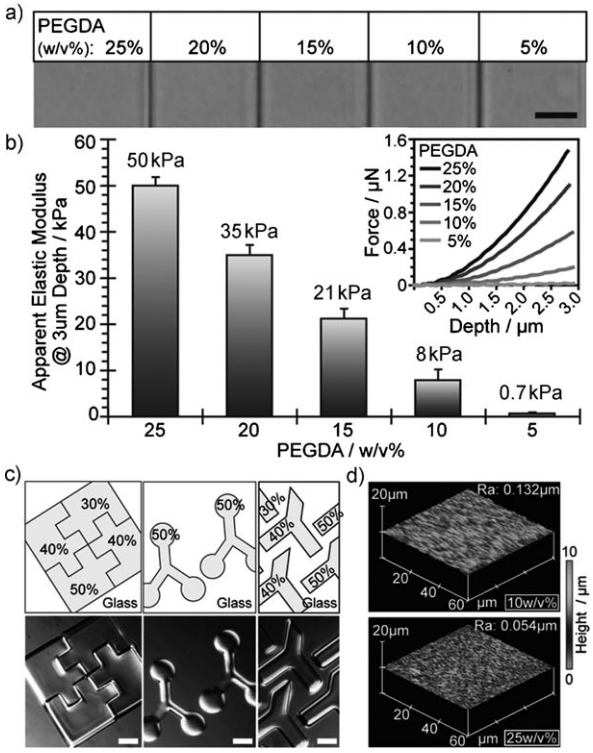

Figure 2. Fabrication of cell-adhesive substrate with discrete heterogeneities, and verification of stiffness. a) A bright-field image of a discrete stiffness gradient, with a constant step size of (130 ± 1) μm. Percentages indicate the w/v% of PEGDA (MW: 4 kDa) added in each section of the gradient. Scale bar: 50 μm. b) Apparent elastic moduli of each section of the gradient as measured by AFM indentation. Data shown are mean ± standard deviation ($n = 32$). Inset: indentation force-response curves for 3 μm indentations on hydrogels of different w/v% of PEGDA. c) Fabrication of freeform stiffness patterns using a confocal laser scanning microscope. 2 mg mL^{-1} of PEG-fibrinogen was added to 30, 40, and 50 w/v% of PEGDA (MW: 400 Da) to yield hydrogels of three different stiffnesses. The upper and lower panels show the schematics and phase-contrast images of three different stiffness patterns, respectively. Percentages denote the w/v% of PEGDA added. All scale bars are 100 μm. d) Contact mode surface scans of hydrogels containing 10 and 25 w/v% of PEGDA and their respective average surface roughness.

across a stiffness boundary (Supporting Information, Figure S3c).

To characterize cell morphology we plated human foreskin fibroblasts (HFFs) on a discrete stiffness gradient of a similar geometry to that in Figure 2a. The HFFs attached and spread along the gradient, and assumed a characteristic spindle-like morphology in 10 h after seeding (Figure 3a). To limit the interference of cell–cell contacts on the stiffness-dependent morphological response[1] we examined cells seeded on a series of hydrogels with uniform stiffness ranging from 8 to 50 kPa at low cell density (10000 cells cm^{-2}). We observed a steady increase in projected cell areas with increasing gel stiffness (Figure 3b). This finding is consistent with previous studies, where cell area increases with gel stiffness (stiffness ranging from 1 to 40 kPa).[1,3,6,18,29] In addition to cell morphology, we examined how the discrete stiffness gradient affected cytoskeleton organization. We

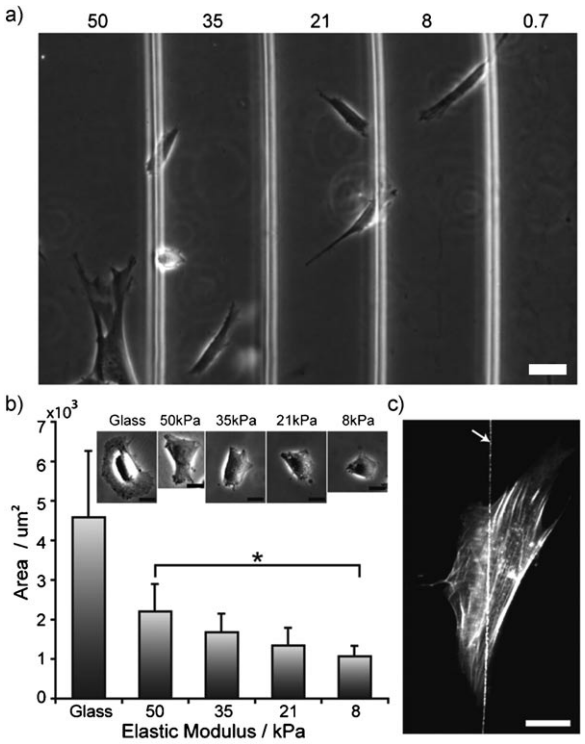

Figure 3. Morphological response and cytoskeleton organization on discrete stiffness gradients. a) HFFs plated on a discrete stiffness gradient for 10 h. Stiffness of each section of the gradient was measured by AFM and is indicated on the top. b) Projected area of cells on separate hydrogels with stiffness ranging from 8 to 50 kPa (10 h after plating, glass surface as reference). Data shown are mean ± standard error of mean ($n = 10$–17). The differences in average projected area among the four groups (50, 35, 21, 8 kPa) were statistically significant, as determined by ANOVA ($p < 0.05$). c) HFFs spanning across a boundary (arrow), with 41 and 37 w/v% of PEGDA on the left and right, respectively, demonstrated well-defined actin stress fibers throughout the cytoplasm. Scale bars are a) 50 μm and b,c) 25 μm.

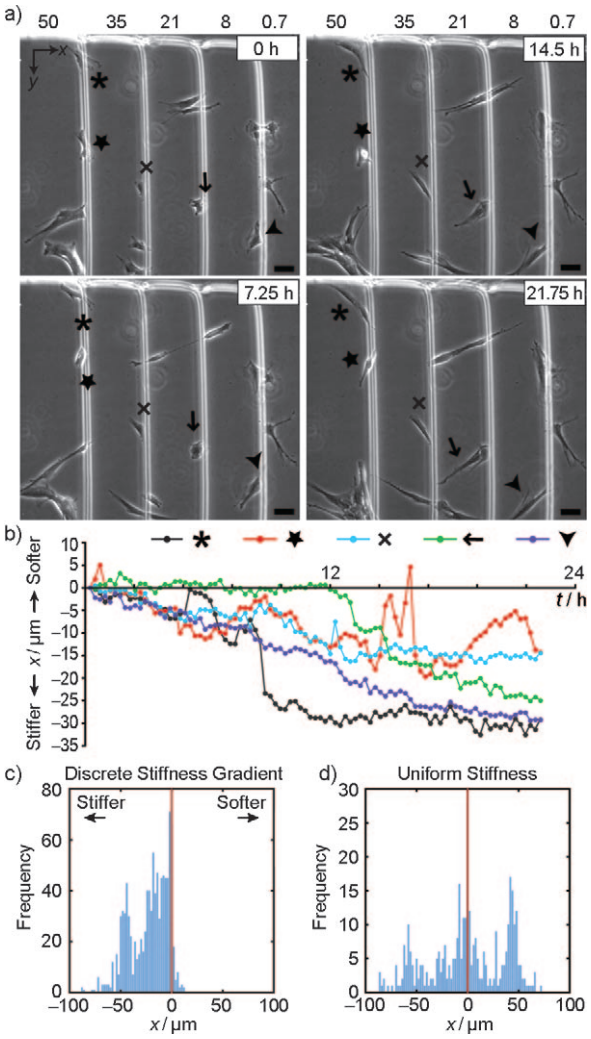

Figure 4. Cell migration on discrete stiffness gradient. a) HFFs were seeded onto a discrete stiffness gradient (uniform step size of ca. 130 μm, 0.7 to 50 kPa) for 10 h after which cell migration was recorded for another 22 h. Cells that were initially interacting with a stiffness boundary and had no apparent cell–cell contact during the recording were denoted with symbols at each selected time point. Elastic moduli (in kPa) of each section of the gradient are shown above. All scale bars are 50 μm. b) Trajectories of cell centroids along the direction of the gradient for each cell denoted in (a). The initial position for each cell is set to $x = 0$. Positive x indicates movement towards the softer regions, and negative x indicates movement towards the stiffer regions. c,d) Histograms of centroid positions (with initial positions set to $x = 0$) of ten cells recorded during 22 h that were initially in contact with stiffness boundaries on two identical discrete stiffness gradients and four cells on two hydrogel patterns with uniform stiffness (Supporting Information, Figure S4). The histograms show the left-shifted distribution of centroid positions of cells on discrete stiffness gradients compared to cells on hydrogel with uniform stiffness, suggesting that cells are preferentially migrating towards the stiffer regions. Red lines denote $x = 0$.

plated HFFs on a discrete stiffness gradient for 10 h, and then fixed and stained the cells for actin filaments. Similar to previous findings,[29] we observed organized actin stress fibers spanning throughout the cytoplasm of a cell adhering across a boundary between two relatively stiff hydrogels (> 100 kPa) (Figure 3c).

Finally, we studied the migration of HFFs on cell-adhesive matrices with discrete heterogeneities in stiffness. We created a discrete stiffness gradient similar to that shown in Figure 2a. The overall gradient in stiffness (ca. 75 Pa μm^{-1}) is within an order of magnitude of the continuous stiffness gradients (ca. 13 Pa μm^{-1}) in previous studies using collagen-coated polyacrylamide gels.[18] We plated HFFs on the gradient at a low cell density of 10000 cells cm^{-2} for 10 h. After 10 h we recorded cell migration using time-lapse microscopy at an interval of 15 min. During the following 22 h, it was observed that 85% of all cells that were initially in contact with a boundary preferentially migrated toward the stiffer regions (Figure 4a and Supporting Information). The directionality of these migrations was evident from examining the trajectories of cell centroids along the direction of the gradient over the course of 22 h (Figure 4b). The distribution of centroid positions (relative to the initial positions) of cells initially interacting with a stiffness boundary was biased toward the stiffer regions of the gradient, whereas that of cells plated on hydrogels with uniform stiffness spread in both directions

(Figure 4c). Taken together, our cell migration data suggest that the cells respond to the patterned stiffness heterogeneity by migrating towards the stiffer regions along the discrete stiffness gradients. This result agrees with previously published data on durotaxis of NIH 3T3 mouse fibroblasts across a single-step stiffness gradient[3] or on a continuous stiffness gradient,[18] where cells demonstrate directional migration towards the stiffer regions.

Although microfluidics-based lithography is a burgeoning tool for fabrication of microstructures, it has thus far focused mostly on the synthesis of polymeric monodisperse microparticles in solution.[30] Based on a previous technology developed in our group, herein we extend the lithographic tool for the fabrication of 3D ECM and control of cellular microenvironments with high precision and flexibility. Compared to previously used materials for controlling substrate stiffness, such as polydimethylsiloxane (PDMS) and polyacrylamide, the use of a composite matrix made from PEG-fibrinogen and PEGDA allows one to pattern cell-adhesive substrates with a range of stiffness and spatial resolution that are observed in native tissues, but have thus far not been reproduced in vitro. Furthermore, a PEG-fibrinogen/PEGDA composite matrix permits mechanotransduction through direct cell–matrix contact, instead of contact through a thin layer of anchored protein on top of an underlying PDMS or polyacrylamide-based substrate. Our approach of using a constant percentage of PEG-fibrinogen should also provide a relatively uniform density of cell adhesion sites across microfabricated gels of different stiffnesses, to facilitate studies for decoupling effects of varying stiffness versus cell adhesion. However, the addition of PEGDA could also increase steric shielding of the PEG-fibrinogen, and further investigation is required to determine the degree of such an effect. Moreover, our approach is suitable for creating microstiffness patterns with non-PEG-based photopolymerizable hydrogels, such as polyacrylamide, methacrylated hyaluronic acid,[31] and photocross-linkable polyvinyl alcohol hydrogels.[32] Overall, we believe that the ability to micropattern cell-adhesive substrates exhibiting well-defined microscale variations in space[33] and in stiffness may allow the testing of hypotheses concerning the role of differential cell-ECM interactions in cell processes, such as adherence, spreading, migration, and differentiation that are fundamental to the normal and pathological function of native biological tissues.

Experimental Section

Fabrication of discrete stiffness gradients: The following method was used herein, except for the results shown in Figure 2c and Figure 3c (Supporting Information), using an epifluorescence microscope. The prepolymer solutions were prepared by mixing a constant amount of PEG-fibrinogen (40 v/v %) with various w/v % of PEGDA (5, 10, 15, 20, or 25 w/v %; MW: 4 kDa; Polysciences, Warrington, PA) in sterile PBS buffer solution. The final protein concentration was 4 mg mL^{-1}. All prepolymer solutions also contained 1 w/v % of 2-hydroxy-1-[4-(2-hydroxyethoxy)phenyl]-2-methyl-1-propanone (Irgacure2959; Ciba, Tarrytown, NY) as the photoinitiator and 1 v/v % of 1-vinyl-2-pyrrolidone as an cross-link accelerator. During each fabrication cycle, a prepolymer solution was drawn into a microfluidic channel (with a height of 90 μm), where it was cross-linked by exposing to the UV light source on a conventional epifluorescence microscope (Leica DMI6000B and EL6000; Leica Microsystems, IL) for 4 to 13 s. The size and shape of the hydrogel blocks were controlled by the power of the objective lens and the dimensions of the field diaphragm. Un-cross-linked material was subsequently removed by a series of buffer washes. A new prepolymer solution was introduced into the microfluidic channel and the fabrication cycle was repeated. We purposely overlapped the UV exposure window in each fabrication cycle to achieve a spatial resolution of 27 μm (Supporting Information, Figure S1). Upon completion of fabrication, the microfluidic channel was peeled away, allowing the hydrogel patterns to equilibrate in sterile PBS buffer solution for at least 24 h to leach out any toxic substances prior to plating of cells.

Characterizing stiffness patterns using AFM: We verified the discrete stiffness gradient of our hydrogel patterns using AFM indentations, and roughness and topography information with AFM imaging. We probed an area of 30×30 μm in the middle of each hydrogel pattern with a 4×4 indentation array (with 10 μm spacing). We determined ('pointwise') the depth-dependent apparent elastic modulus for each indentation as previously described.[34] For detailed procedure, see the Supporting Information.

Image analysis for projected cell area and cell migration: We took phase-contrast images of seeded cells on different regions of a stiffness pattern with a 10x phase objective lens. Images were processed and analyzed using ImageJ software (National Institutes of Health). To measure projected cell area, we manually segmented individual cells in each image and measured the segmented area using ImageJ. We performed one-way ANOVA tests to determine statistical significance of differences between more than two groups of samples. For cell migration data, time-lapse images of selected cells (those that did not appear to demonstrate cell–cell contact and were either in contact with stiffness boundaries or were seeded on hydrogel of uniform stiffness) were segmented and tracked for centroid positions using ImageJ. Further data analyses were performed using MATLAB (MathWorks, Natick, MA).

Received: February 10, 2009
Published online: May 28, 2009

Keywords: hydrogels · mechanosensing · microfabrication · micofluidics · polymerization

[1] T. Yeung, P. C. Georges, L. A. Flanagan, B. Marg, M. Ortiz, M. Funaki, N. Zahir, W. Ming, V. Weaver, P. A. Janmey, *Cell Motil. Cytoskeleton* **2005**, *60*, 24.
[2] R. J. Pelham, Jr., Y. Wang, *Proc. Natl. Acad. Sci. USA* **1997**, *94*, 13661.
[3] C. M. Lo, H. B. Wang, M. Dembo, Y. L. Wang, *Biophys. J.* **2000**, *79*, 144.
[4] D. Dikovsky, H. Bianco-Peled, D. Seliktar, *Biophys. J.* **2008**, DOI: biophysj.107.105841.
[5] H. B. Wang, M. Dembo, Y. L. Wang, *Am. J. Physiol. Cell Physiol.* **2000**, *279*, C1345.
[6] A. J. Engler, S. Sen, H. L. Sweeney, D. E. Discher, *Cell* **2006**, *126*, 677.
[7] J. Alcaraz, R. Xu, H. Mori, C. M. Nelson, R. Mroue, V. A. Spencer, D. Brownfield, D. C. Radisky, C. Bustamante, M. J. Bissell, *EMBO J.* **2008**, *27*, 2829.
[8] M. J. Paszek, N. Zahir, K. R. Johnson, J. N. Lakins, G. I. Rozenberg, A. Gefen, C. A. Reinhart-King, S. S. Margulies, M. Dembo, D. Boettiger, D. A. Hammer, V. M. Weaver, *Cancer Cell* **2005**, *8*, 241.
[9] M. A. Wozniak, P. J. Keely, *Biol. Proced. Online* **2005**, *7*, 144.
[10] B. S. Elkin, E. U. Azeloglu, K. D. Costa, B. Morrison III, *J. Neurotrauma* **2007**, *24*, 812.

[11] J. Y. Rho, P. Zioupos, J. D. Currey, G. M. Pharr, *J. Biomech.* **2002**, *35*, 189.
[12] G. Balooch, M. Balooch, R. K. Nalla, S. Schilling, E. H. Filvaroff, G. W. Marshall, S. J. Marshall, R. O. Ritchie, R. Derynck, T. Alliston, *Proc. Natl. Acad. Sci. USA* **2005**, *102*, 18813.
[13] E. A. Zamir, V. Srinivasan, R. Perucchio, L. A. Taber, *Ann. Biomed. Eng.* **2003**, *31*, 1327.
[14] J. K. Rains, J. L. Bert, C. R. Roberts, P. D. Pare, *J. Appl. Physiol.* **1992**, *72*, 219.
[15] K. K. Parker, D. E. Ingber, *Philos. Trans. R. Soc. London Ser. B* **2007**, *362*, 1267.
[16] H. B. Wang, M. Dembo, S. K. Hanks, Y. Wang, *Proc. Natl. Acad. Sci. USA* **2001**, *98*, 11295.
[17] J. Y. Wong, A. Velasco, P. Rajagopalan, Q. Pham, *Langmuir* **2003**, *19*, 1908.
[18] N. Zaari, P. Rajagopalan, S. Kim, A. Engler, J. Wong, *Adv. Mater.* **2004**, *16*, 2133.
[19] D. C. Pregibon, M. Toner, P. S. Doyle, *Langmuir* **2006**, *22*, 5122.
[20] Y. K. Cheung, B. Gillette, M. Z. Zhong, S. Ramcharan, S. K. Sia, *Lab Chip* **2007**, *7*, 574.
[21] Y. K. Cheung, D. Shiovitz, S. K. Sia in *Lab on a Chip Technologies and Applications* (Eds.: K. E. Herold, A. Rasooly), Horizon Scientific Press, in press.
[22] S. A. Lee, S. E. Chung, W. Park, S. H. Lee, S. Kwon, *Lab Chip* **2009**, in press.
[23] P. Panda, S. Ali, E. Lo, B. G. Chung, T. A. Hatton, A. Khademhosseini, P. S. Doyle, *Lab Chip* **2008**, *8*, 1056.
[24] L. Almany, D. Seliktar, *Biomaterials* **2005**, *26*, 2467.
[25] A. S. Gobin, J. L. West, *Faseb J.* **2002**, *16*, 751.
[26] S. Halstenberg, A. Panitch, S. Rizzi, H. Hall, J. A. Hubbell, *Biomacromolecules* **2002**, *3*, 710.
[27] D. L. Hern, J. A. Hubbell, *J. Biomed. Mater. Res.* **1998**, *39*, 266.
[28] K. D. Costa, A. J. Sim, F. C. Yin, *J. Biomech. Eng.* **2006**, *128*, 176.
[29] A. Engler, L. Bacakova, C. Newman, A. Hategan, M. Griffin, D. Discher, *Biophys. J.* **2004**, *86*, 617.
[30] R. S. Kane, *Angew. Chem.* **2008**, *120*, 1388; *Angew. Chem. Int. Ed.* **2008**, *47*, 1368.
[31] J. A. Burdick, C. Chung, X. Jia, M. A. Randolph, R. Langer, *Biomacromolecules* **2005**, *6*, 386.
[32] R. H. Schmedlen, K. S. Masters, J. L. West, *Biomaterials* **2002**, *23*, 4325.
[33] B. M. Gillette, J. A. Jensen, B. Tang, G. J. Yang, A. Bazargan-Lari, M. Zhong, S. K. Sia, *Nat. Mater.* **2008**, *7*, 636.
[34] K. D. Costa, *Methods Mol. Biol.* **2006**, *319*, 331.

